Journal of Thermal Analysis and Calorimetry, Vol. 73 (2003) 715–725

SOLVATES WITH ANOMALOUS LOW MELTING POINTS
Preparation, structural and thermochemical aspects

G. L. Perlovich [1,3], *L. Kr. Hansen* [2] *and A. Bauer-Brandl* [1*]

[1]University of Tromsø, Institute of Pharmacy, Breivika, 9037 Tromsø, Norway
[2]University of Tromsø, Institute of Chemistry, Breivika, 9037 Tromsø, Norway
[3]Institute of Solution Chemistry, Russian Academy of Sciences, 153045 Ivanovo, Russia

(Received August 28, 2002; in revised form February 20, 2003)

Abstract

Single crystals of the N,N-dimethylformamide (DMF) solvate (1:1) of flurbiprofen (FBP) were grown for the first time and characterised by X-ray diffraction, IR spectrophotometry, DSC and solution calorimetric methods. The structure may be characterised as a layer-structure, where DMF double-sheets are arranged between FBP double-sheets. The FBP and DMF molecules are linked to each other by a hydrogen bond, which is formed between the hydroxyl group of FBP and the carbonyl group of DMF. The conformation of FBP molecules in the DMF solvate differs from analogous enantiomers in the unsolvated form. The differences are discussed from the point of view of the influence of the nature of the solvent on selective crystallisation of the enantiomers. A peculiarity of the solvate is its low melting point, 37.3±0.2°C, with respect to the unsolvated phase, 113.5±0.2°C. Based on solution enthalpies of the solvated and unsolvated phases dissolved in DMF, the difference in crystal lattice energies, 9.8 kJ mol^{-1}, was calculated and the difference in entropies, 33 J mol^{-1} K^{-1} estimated. A possible mechanism explaining the low melting point of the solvate is discussed.

Keywords: conformational state, crystal lattice energy, crystal structure, DSC, enantiomers, enthalpy of fusion, enthalpy of solution, entropy, flurbiprofen, IR-spectrum, melting point, solvate, X-ray

Introduction

A crucial aspect in the design of drug preparations is delivery of the active substance to the sites of action. This is particularly problematic with substances slowly dissolving, whereof flurbiprofen (FBP) is not an exception [1, 2]. Several approaches to solve this problem have been described: firstly, the polymorphic modification with the lowest crystal lattice energy [3, 4] can be chosen. Another way is to create inclusion complexes between cyclodextrins and FBP [5–9].

* Author for correspondence: E-mail: annetteb@farmasi.uit.no

1388–6150/2003/ $ 20.00
Akadémiai Kiadó, Budapest

A new approach to overcome the problem of delivery of drugs is the design of solvates [drug+guest] with a melting point approximately at body temperature. Of course, choice of solvent (guest) should essentially be focused on toxicity and safety. However, at this time, it is the purpose of the present paper to show the hypothetical opportunity of the existence of such pharmaceutical systems. It is an attempt to demonstrate the proposed approach exemplified by solvate phase of [FBP+DMF], the melting point of which is at body temperature. (Melting process in this context implies the phase transition between a solid phase (i.e. the solvate [FBP+DMF]) and a liquid phase (i.e. FBP solute in DMF)). This system may hypothetically be useful for a transdermal formulation of the antiinflammatory drug substance Flurbiprofen comprising DMF as an absorption enhancer. In the delivery process, not only single drug-molecules may take part, but drug+solvent like a solvation shell.

The present paper focuses at structure and thermochemical properties of the DMF- solvate of flurbiprofen.

Experimental

Materials and solvents

The studies of flurbiprofen (FBP) ([±]-2-fluoro-α-methyl-4-biphenylacetic acid, $C_{15}H_{13}FO_2$, MW 244.3) were carried out using the commercial product from Sigma Chemical Co., St. Louis, USA (lot 38H1398). The crystal solvate [FBP+DMF] was grown using the N,N-dimethylformamide (DMF) of analytical reagent grade from Sigma Chemical Co., St. Louis, USA (lot 11K1321).

Preparation of the crystals

The FBP crystals were grown from saturated acetone solution by slow evaporation.

The solvate was obtained as follows: into a saturated solution of FBP in DMF, water was carefully added drop by drop until a homogeneous nucleation looking like a white muddy precipitation was observed. (The water drops added to (FBP+DMF) solution promote the creation of a few nuclei, because FBP is insoluble in water.) Afterwards, the solution was left in a saturated water vapour atmosphere at room temperature. This method is similar to the method described by Guillory [10]. Saturation of the solution by water vapour promotes 'soft' (slow) growth of the existing nuclei. Single crystals grew within 24 h. All experiments with the crystals were carried out within 8 h after harvesting them from the solution.

Thermoanalytical methods

Differential scanning calorimetry (DSC) measurements for FBP and [FBP+DMF] were carried out in the temperature interval from –150 to 130°C using a Perkin Elmer Pyris 1 DSC differential scanning calorimeter (Perkin Elmer Analytical Instruments, Norwalk, Connecticut, USA) and Pyris software for Windows NT. DSC runs were performed in an atmosphere of flowing (20 mL min^{-1}) dry argon gas of high purity 99.990% using stan-

dard aluminium sample pans with both closed and perforated lids. The DSC was calibrated with indium from Perkin Elmer (P/N 0319-0033). The value for enthalpy of fusion corresponded to 28.48 J g^{-1} (reference value 28.45 J g^{-1}). The melting point was 156.5±0.1°C (n=10). All the DSC-experiments were carried out at various heating rates 2, 5, 10, 15, 20 K min^{-1}. The accuracy of mass measurements was ±0.0005 mg.

Solution Calorimetry. Enthalpies of solution (ΔH_{sol}) at a concentration m were measured using a Precision Solution Calorimeter in the 2277 Thermal Activity Monitor Thermostat (both from Thermometric AB, Järfälla, Sweden). The software SolCal Version 1.2 (Thermometric) was applied to all calculations. The measuring temperature was 25.0±10^{-4}°C, volume of the vessel 100 mL, stirrer speed 500 rpm and the mass of the sample approximately 18 mg measured with an accuracy of ±0.0005 mg. The number of samples of each of the respective phases was not less than 5, depending on the reproducibility of the results. The calorimeter was calibrated using KCl (analytical grade >99.5%, from Merck) in water in a wide concentration interval (sample mass between 18 and 100 mg) with more than 10 measurements. The standard value of solution enthalpy obtained was ΔH^0_{sol}=17225±50 J mol^{-1}. This is in good agreement with the value recommended by IUPAC of ΔH^0_{sol}=17217±33 J mol^{-1} [11].

Spectroscopic method

IR spectra were recorded with a Perkin Elmer 1600 FT-IR spectrophotometer. Samples were scanned in the form of potassium bromide pellets at a resolution of 4 cm^{-1}.

X-ray measurement

Single-crystal X-ray measurements were carried out using a Nonius CAD-4 diffractometer with graphite-monochromated MoK_α radiation (λ=0.71069 Å). Intensity data were collected at 25°C by means of an ω-2θ scanning procedure up to 2θ=48° (for [FBP+DMF]) and 50° (for the FBP). The crystal structure was solved using direct methods and refined by means of a full-matrix least-squares procedure. All programs used for the solution, refinement and display of the structures are included in the *OSCAIL* program package [12]. *CAD-4 Software* [13] was applied for data collection, data reduction and cell refinement. Programs *SHELXS-97* [14] and *SHELXL-97* [15] were used to solve and to refine structures, respectively.

Results and discussion

Structural aspects

The crystal structure of unsolvated FBP has been described earlier [16]. However, in order to enable a detailed comparison of the unsolvated and solvated phases, another FBP crystal was grown and its structure was re-determined once more. The results of the X-ray analyses between published data and our data of FBP and between solvated and unsolvated phases are compared in Table 1.

Table 1 Parameters crystal lattices of FBP and [FBP+DMF] solvate[a]

	FBP[b]	FBP	[FBP+DMF]
Crystal data			
crystal system	triclinic	triclinic	monoclinic
space group	$P\bar{1}$	$P\bar{1}$	P *n*
description		Colourless block	Colourless plate
crystal size, mm	0.05×0.08×0.50	0.60×0.50×0.40	0.30×0.20×0.15
a/Å	9.315(4)	9.299(3)	5.986(5)
b/Å	12.734(9)	12.721(4)	23.757(12)
c/Å	5.823(2)	5.786(5)	6.275(4)
α/°	83.0(1)	82.99(4)	90.00
β/°	107.2(1)	107.28(4)	108.51(4)
γ/°	107.0(1)	106.94(3)	90.00
volume/Å^3	630(1)	624.7(6)	846.2(10)
Z	2	2	2
D_{calc}/ g cm^{-3}	1.29	1.293	1.246
radiation[c]	CuK_α	MoK_α	MoK_α
T/°C	25(2)	25(2)	25(2)
μ/mm^{-1}		0.095	0.092
Data collection			
measured reflections	1953	2460	1452
independent reflections		2170	1434
independent reflections with>2σ(I)	955	1716	449
R_{int}		0.0118	0.0053
θ_{max}/°		24.98	23.99
Refinement			
refinement on	F^2	F^2	F^2
R $F^2>2\sigma(F^2)$	0.062	0.0378	0.0659
ω*R*(F^2)		0.1185	0.2416
S		1.076	0.814
reflections		2170	1434
parameters		221	221
$(\Delta/\sigma)_{max}$		0.003	0.101
$\Delta\rho_{max}$, e·Å^{-3}		0.185	0.253
$\Delta\rho_{min,}$ e·Å^{-3}		–0.158	–0.310
extinction correction		SHELXL[d]	SHELXL[d]
extinction coefficient		0.028(8)	0.013(12)

[a]In brackets display the standard deviations; [b][16]; [c]MoK_α (λ=0.71069 Å); CuK_α (λ=1.54178 Å); [d][15]

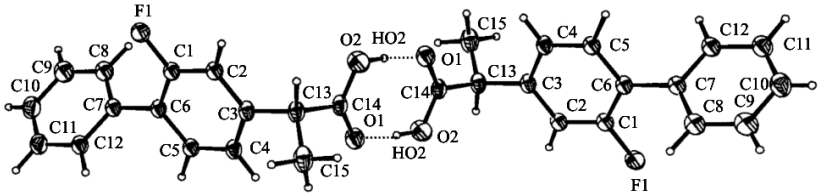

Fig. 1 The structure of a FBP dimer and the atomic numbering scheme. Displacement ellipsoids of non-H atoms are drawn at the 20% probability level

In contrast to the data published by Flipen *et al*. [16], the present FBP crystal was of very good quality, which enabled to obtain co-ordinates of the H-atoms from experimental data and to describe the geometry of the hydrogen bonds in more detail. In the crystal of FBP, the molecules are packed as dimers (Fig. 1). Hydrogen-bonding geometry of FBP for both cases is presented in Table 2.

Table 2 Hydrogen-bonding geometry of FBP and [FBP + DMF] solvate[a]

	D—H···A	D—H/Å	H···A/Å	D···A/Å	D—H···A/°
FBP[b]	O2–HO2···O1[ic]	1.29(6)	1.36(7)	2.655(6)	174.7(4)
FBP		1.02(3)	1.62(4)	2.643(2)	178.3(3)
[FBP+DMF]	O2–H1···O3	0.82(10)	1.8(2)	2.6(2)	165(5)

[a] In brackets display the standard deviations; [b] [16]; [c] Symmetry code: (i) $1 - x$, $2 - y$, $1 - z$

In the present study the hydrogen atom is found to be localised closer to atom O2 and the distance O1(sym. cod 1–x, 2–y, 1–z)···HO2 to be longer compared to earlier publications. Analogous phenyl fragments of neighbouring molecules are stacked face-to-face at distances between the coplanar planes of 3.93(5) and 5.17(5) Å, respectively. These values are slightly bigger in comparison to the values for the local energetic minimum calculated for benzene dimers (3.85 Å) [17, 18]. Probably, the steric hindrances and the hydrogen bonding between FBP and DMF molecules explain this fact. The adjacent phenyl rings of a FBP molecule are tilted around the C6-C7 bond by 53.5(4)°.

As follows from X-ray diffraction, the [FBP+DMF] solvate has a 1:1 stoichiometry. In contrast to unsolvated FBP, the F-atoms in positions 2- (with respect to C6) are disordered in the DMF-solvate (Fig. 2). This means that the peaks found for F11 are a combination of 70% fluorine and 30% hydrogen peaks, whereas for F12 this proportion is 30 and 70%, respectively. To simplify analysis of the conformation states, it is supposed that the F atom is situated mainly in the position with the maximum value of peak occupation. (Below only one fluorine position is discussed.)

The conformation state of the FBP molecule in the DMF solvate differs from the unsolvated form. Let one look at the molecule along C6-C7 bond from the $–CHCH_3COOH$ substituent in *para*- position (the non-substituted phenyl fragment, Ph_1, is pointing upwards) (Fig. 3). This approach is introduced in order to simplify compari-

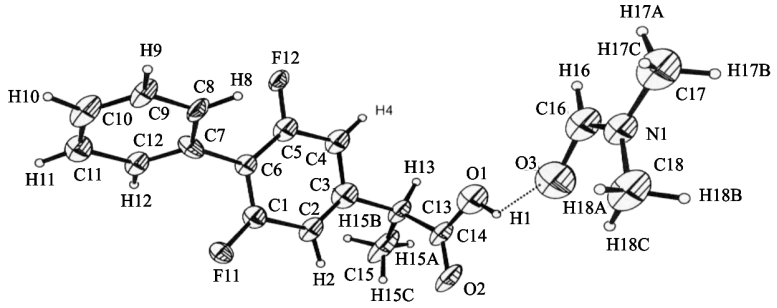

Fig. 2 The molecular structure of the [FBP+DMF] solvate and the atomic numbering scheme. Displacement ellipsoids of non-H atoms are drawn at the 20% probability level (F12 and F11 disordered F-atom, see text)

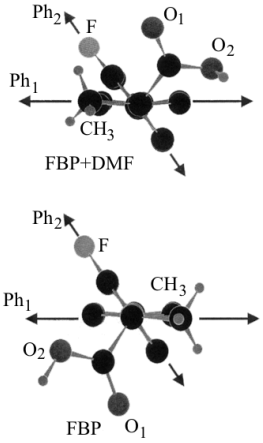

Fig. 3 A view of analogous enantiomers in the solvated [FBP+DMF] and in the unsolvated FBP along the C6-C7 bond from the –$CHCH_3COOH$ substituent in *para*- position (the non-substituted phenyl fragment, Ph_1, is pointing upwards)

son of the conformation states. The torsion angle between the plane of the terminal phenyl motif (Ph_1) and groups F, CH_3, COOH is defined clockwise. For solvate (S) the torsion angle (Ph_1; C-CH_3) or C12-C7-C13-C15 is 1(1)°, whereas for the unsolvated crystal (UC) it is 4.4(4)° (for the same enantiomers). The torsion angle (Ph_1; C-COOH) or C12-C7-C13-C14 is 125(1)° (S) and 304.5(4)° (UC), respectively. Torsion angle (Ph_1; C-F) or C12-C7-C6-C1 is 52.2(18)° (S) compared to 53.5(4)° (UC). The essential difference between the considered isomers is: a) in the solvate, the carboxyl group is situated on the same side of Ph_1 as the fluorine atom, whereas for the unsolvated crystal – on the opposite side. (However, it should be noted that for both enantiomers the carboxyl group is situated in the biggest sector between adjacent phenyl planes); b) in both cases the methyl groups are arranged approximately in the Ph_1 planes. Therefore, it may be supposed that in the solution, the DMF molecules form a particular solvation shell, which induces a special conformation of the FBP molecule (for the same enantiomer), which is different from the conformation in the unsolvated crystal. This fact illustrates once more

the influence of the nature of the solvent on selective crystallisation of special conformation states of enantiomers [19, 20].

Phenyl fragments of FBP form two packing types: face-to-face (with distances between neighbouring molecules being 5.981(2) and 6.267(2) Å) and T-shape. Hydrogen bonds between DMF and FBP molecules are described by the following parameters: O3···H1 is 1.8(2) Å; O3···O2 is 2.6(2) Å; O2-H1···O3 is 165(5)°. Packing of molecules in the DMF solvate of FBP may be characterised as a layer-structure: DMF double-sheets lie between FBP double-sheets (Fig. 4). Moreover, the DMF sheet interacts with the FBP sheet by both van der Waals interactions and hydrogen bonds, while the adjacent DMF sheet interacts only by the van der Waals interaction through contacting methyl groups. In contrast to the solvate discussed above, the FBP unsolvated crystal lattice is built from dimeric aggregates, which interact with each other by effective (from the point of view of anisotropic van der Waals interactions) adjacent bi-phenyls contacts. Moreover, planes of the bi-phenyl fragment are situated approximately perpendicular to the hydrogen bonds. The examined situation, from a general point of view, is similar to the difference between α- and β-modifications of glycine [21].

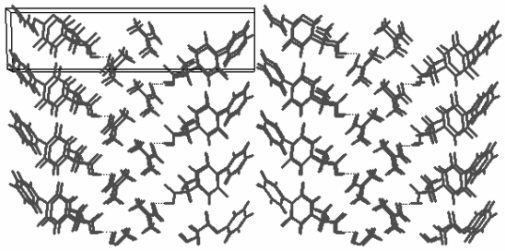

Fig. 4 A detail of the packing of molecules in the lattice of the [FBP+DMF] solvate depicted in c-direction

The most significant part of IR spectra of the unsolvated and solvated phases is shown in Fig. 5. For unsolvated FBP a distinct absorption band at 1700 cm^{-1} is observed

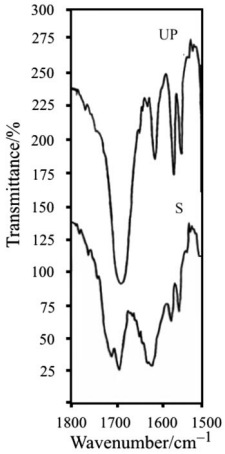

Fig. 5 Details of the IR spectra of the solvated (S) and unsolvated (UP) phases of FBP

which corresponds to the carbonyl C14=O1 stretching vibrations. On the other hand, the analogous band for the solvated phase is split into two peaks at 1718 and 1700 cm^{-1}. Therefore, it may be supposed that the high frequency band of the split is connected to the carbonyl group, which does not take part in creation of a hydrogen bond, C14=O1. The low frequency absorption band corresponds to C16=O3 stretching vibrations of DMF that forms a hydrogen bond with the OH-group of FBP (Fig. 2). As follows from X-ray analysis, the lengths and geometry of the intermolecular hydrogen bonds both of the solvated and unsolvated phases are approximately equal, which corresponds to equal interaction energy. This is confirmed by the coincidence of carbonyl stretching vibrations of FBP molecule in the unsolvated phase and DMF molecule in the solvate. Based on the proposed considerations, it may be supposed that the polymorphic modification II of unsolvated FBP which was described by Henk *et al*. [3] (with C=O stretching vibrations at 1715 cm^{-1}) and Lacoulonche *et al.* [4] (1711 cm^{-1}) consists of molecules which do not form dimeric structures.

DSC measurements

The results of the DSC measurements are shown in Table 3. It should be noted that both for powder and single crystals no heat effects connected with phase transitions in the interval between –150 and –50°C were observed. The unsolvated FBP melts at 113.5±0.2°C (heating rate 10 K min^{-1}) with an enthalpy of melting of ΔH_f =108 ±2 J g^{-1}=26.4±0.5 kJ mol^{-1}. After cooling the melt down to –50°C in the pan at 10 K min^{-1} and heating again at the same rate, several heat effects are monitored. First of all, at –16.5±0.4°C glass transition, Q_g, is observed. Secondly, the exothermic heat effect at around 45°C corresponds to recrystallisation, Q_{rec}, of FBP from the amorphous state (Fig. 6).

Table 3 The results of thermochemical measurements

Phases	Melting point[a]/°C	Enthalpy of fusion[a]/J g^{-1}	Solution enthalphy[b]/ kJ (mol FBP)$^{-1}$
FBP	113.5±0.2	108±2	7.2±0.1
[FBP+DMF]	37.3±0.3	70±2	17.0±0.3

[a]heating rate 10 K min^{-1}; n =10 ; [b]n = 5–7

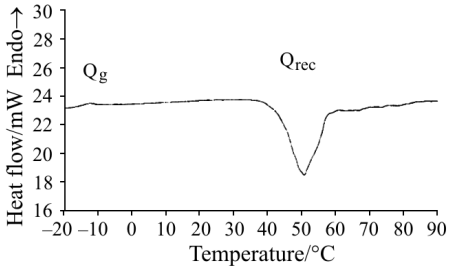

Fig. 6 DSC curves of the amorphous FBP, obtained by melting and subsequent cooling of the melt down to –50°C in the same pan (heating and cooling rates: 10 K min^{-1})

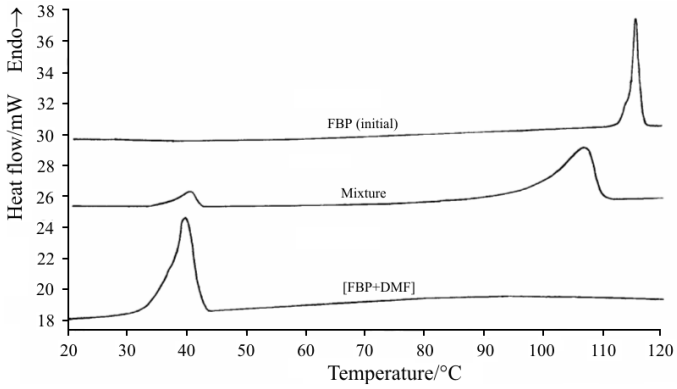

Fig. 7 DSC curves of the initial FBP, [FBP+DMF] solvate and a mixture thereof (see text); heating rate: 10 K min^{-1}

Freshly prepared crystals of [FBP+DMF] melt at 37.3°C and the heat effect is 70 J g^{-1} (Fig. 7). The solvate mass loss with heating to 120°C is 7% (determined by the mass difference before and after DSC measurement in the open pan), which is about 30% of total DMF content in the solvate. The enthalpy of melting is not altered by different heating rates (2, 5, 10, 15, 20 K min^{-1}). However, the temperature interval, at which it is observed, essentially is widened with increasing heating rates. It should be emphasised that the onset temperatures of the effects are practically the same independently of the heating rate; this does not correspond to the typical behaviour of DSC curves for desolvation processes, where the onset temperature is shifted to a higher temperature when the heating rate is increased. Since, it may be assumed that the observed heat effect is a consequence of the superposition of several processes going on in the crystal lattice.

Solution calorimeter measurements

In order to compare the difference between crystal lattice energies of the solvated (S) and unsolvated phase (UP) of FBP, solution calorimetry experiments were carried out in the same solvent - DMF. It is well known [22] that:

$$[\text{FBP+guest}]+n\text{Solvent}\rightarrow$$

$$\text{FBP}\cdot m\cdot\text{Solvent}+\text{guest}\cdot l\cdot\text{Solvent}+(n\text{-}m\text{-}l)\cdot\text{Solvent}+\Delta H^0_{\text{sol}}(\text{S}) \quad (1)$$

$$[\text{FBP}]+n\cdot\text{Solvent}\rightarrow\text{FBP}\cdot m\cdot\text{Solvent}+(n\text{-}m)\cdot\text{Solvent}+\Delta H^0_{\text{sol}}(\text{UP}) \quad (2)$$

$$\Delta\Delta H^0_{\text{sol}}(\text{FBP}\rightarrow[\text{FBP+DMF}])=\Delta H^0_{\text{sol}}(\text{S})-\Delta H^0_{\text{sol}}(\text{UP}) \quad (3)$$

where guest is guest molecule of solvate (DMF); Solvent is DMF; n is a number of molecules of the pure solvent; m is a number of the solvent molecules into the solvation shell of FBP in the solution; l is a number of the solvent molecules into the solvation shell of the guest-molecule in the solution.

The results of calorimetric measurements are presented in Table 3. As follows from Table 3, the crystal lattice energy (absolute value) of [FBP+DMF] is higher than that of the unsolvated phase FBP; the difference $\Delta\Delta H^0_{sol} = 9.8 \pm 0.4$ kJ mol^{-1}. Effects of 'stabilization' of the crystal lattice consisting of host molecules due to accommodation of guest molecules in clathrate and inclusion compounds were described before [23, 24].

During crystallisation of the solvate, it was observed that the solvate [FBP+DMF] often grows simultaneously together with the unsolvated phase, like competitive. Based on this fact, the difference of the entropic terms of the two phases may be estimated by assuming their Gibbs energies to be equal:

$$\Delta G^0_{cr}\ (S) = \Delta G^0_{cr}(UP) \quad (4)$$

$$\Delta H^0_{sol}(S) - T\Delta S^0_{sol}(S) = \Delta H^0_{sol}\ (UP) - T\Delta S^0_{sol}(UP) \quad (5)$$

$$\Delta S^0(UP \rightarrow S) = \Delta S^0_{sol}(S) - \Delta S^0_{sol}(UP) = (\Delta H^0_{sol}(S) - \Delta H^0_{sol}(UP))/T \approx 33 \text{ J mol}^{-1} \text{ K}^{-1} \quad (6)$$

Using the GEPOL program [25] and Kitaigorodsky's atomic radii [26] for the calculation of van der Waals volumes (V^w) of the studied molecules, the free volume per one molecule in the unit cell (V^{free}) may be estimated as well as the packing coefficient (K): K(S)=70.91%; K(UP)=72.08%; V^{free}(FBP in S)=92.7 Å^3; V^{free}(FBP in UP)=87.6 Å^3. The obtained data confirm again that the solvated phase has a higher value of entropy.

It should be mentioned that in some cases of crystallization of the solvated phase, yet another (in comparison to the one characterised above) competitive unsolvated phase with a melting point of 96°C was obtained. The DSC curve of a mixture of the solvated and the mentioned unsolvated phase is presented in Fig. 7. Probably this phase corresponds to the crystal modification II of FBP, which was obtained from a saturated *n*-heptane solution by rapid cooling to –18°C and described elsewhere [3, 4] and had the same melting point. We could not grow this phase according to the noted protocol. It should be mentioned that during storage (more than two weeks) at room temperature in air, modification II transformed to the initial phase of FBP (mod. I). Therefore, it may be supposed that the lower melting point of mod. II (with respect to mod. I) is connected to the absence of the hydrogen bonds. This is in good agreement with Li's [27] concept about a correlation between the melting point and the Coulombic term of crystal lattice energy (which is connected not only to a pure Coulombic interaction, but also to the presence of hydrogen bonds).

* * *

This work was generously supported by Norges Forskningsråd, project number HS 58101.

References

1 C. D. Bevan and R. S. Lloyd, Anal. Chem., 72 (2000) 1781.
2 J. Hadgraft, J. Plessis and C. Goosen, Int. J. Pharm., 207 (2000) 31.
3 J. O. Henck and M. Kuhnert-Brandstätter, J. Pharm. Sci., 88 (1999) 103.

4 F. Lacoulonche, A. Chauvet and J. Masse, Int. J. Pharm., 153 (1997) 167.
5 K. Harata, K. Uekama, M. Otagiri and F. Hirayama, J. Incl. Phen., 1 (1984) 279.
6 K. Harata, K. Uekama, T. Imai, F. Hirayama and M. Otagiri, J. Incl. Phen., 6 (1988) 443.
7 K. Uekama, F. Hirayama, T. Imai, M. Otagiri and K. Harata, Chem. Pharm. Bull., 31 (1983) 3363.
8 K. Uekama, T. Imai, F. Hirayama, M. Otagiri and K. Harata, Chem. Pharm. Bull., 32 (1984) 1662.
9 K. Harata, F. Hirayama, T. Imai, K. Uekama and M. Otagiri, Chem. Lett., (1984) 1549.
10 J. K. Guillory, Generation of polymorphs, hydrates, solvates, and amorphous solids. In Brittain H. G., Ed. Polymorphism in Pharmaceutical Solids. New York: Marcel Dekker Inc. 1999, p. 183.
11 J. D. Cox and and G. Pilcher, Thermochemistry of organic and organometallic compounds, London, Academic Press 1970, p. 643.
12 P. McArdle, J. Appl. Cryst., 26 (1993) 752.
13 Enraf-Nonius. 1989. CAD-4 Software. Version 5.0. Enraf-Nonius, Delft, The Netherlands
14 G. M. Sheldrick, SHELXS-97 Program for Crystal Structures Solution. University of Göttingen, Göttingen 1997.
15 G. M. Sheldrick, SHELXL-97 Program for the Refinement of Crystal Structures. University of Göttingen, Göttingen 1997.
16 J. L. Flippen and R. D. Gilardi, Acta Cryst., B31 (1975) 926.
17 P. Hobza, H. L. Selzle and E. W. Schlag, J. Phys. Chem., 97 (1993) 3937.
18 P. Hobza, H. L. Selzle and E. W. Schlag, J. Am. Chem. Soc., 116 (1994) 3500.
19 E. L. Eliel, S. H. Wilen and L. N. Mander, Stereochemistry of organic compounds; John Wiley & Sons, New York 1994.
20 Z. J. Li and D. J. W. Grant, J. Pharm. Sci., 86 (1997) 1073.
21 G. L. Perlovich, L. Kr. Hansen and A. Bauer-Brandl, J. Therm. Anal. Cal., 66 (2001) 699.
22 D. J. W. Grant and T. Higuchi, Solubility behavior of organic compounds. New York, Wiley, 1990.
23 A. Gavezzotti and G. Filippini, Energetic aspects of crystal packing: Experimental and computer simulations. In Gavezzotti A. Ed., Theoretical aspects and computer modelling of the molecular solid state. New York, John Wiley & Sons 1997, pp. 61–97.
24 C. H. Gu and D. J. W. Grant, J. Pharm. Sci., 90 (2001) 1277.
25 J. L. Pascual-Ahuir and E. Silla, J. Comp. Chem., 11 (1990) 1047.
26 A. I. Kitaigorodsky, The molecular crystals. M. Nauka, 1971.
27 Z. J. Li, W. H. Ojala and D. J. W. Grant, J. Pharm. Sci., 90 (2001) 1523.